Photoluminescence Spectral Reliance on Aggregation Order of 1,1-Bis(2′-thienyl)-2,3,4,5-tetraphenylsilole

Junwu Chen,*,† Bin Xu,† Kaixia Yang,† Yong Cao,*,† Herman H. Y. Sung,‡ Ian D. Williams,‡ and Ben Zhong Tang‡

Institute of Polymer Optoelectronic Materials & Devices, Key Laboratory of Specially Functional Materials and Advanced Manufacturing Technology of MoE, South China University of Technology, Guangzhou 510640, China, and Department of Chemistry, Hong Kong University of Science & Technology, Clear Water Bay, Kowloon, Hong Kong, China

Received: April 11, 2005; In Final Form: July 25, 2005

1,1-Bis(2′-thienyl)-2,3,4,5-tetraphenylsilole (**1**) was prepared and characterized crystallographically. Silole **1** exhibited aggregation-induced emission (AIE) behavior like other 2,3,4,5-tetraphenylsiloles. Unexpectedly, aggregates formed in water/acetone (6:4 by volume) mixture emitted a blue light that peaked at 474 nm, while aggregates formed in the mixtures with higher water fractions emitted green light that peaked at 500 nm. Transmission electron microscopy demonstrated that the aggregates formed in the mixture with water fraction of 60% were single crystals, while aggregates that formed in the mixture with water fraction of 90% were irregular and poorly ordered particles. The unusual PL spectral reliance on aggregation order was further confirmed by PL emissions of macroscopic crystal powders and amorphous powders of the silole in the dry state. PL spectral blue shifting was observed upon aging of the poorly ordered aggregates formed in mixtures with water fractions of 70−90%, and they finally exhibited the same blue emission as the crystalline aggregates. The as-deposited thin solid film was amorphous and it could be transformed to a transparent crystalline film upon treatment in the vapor of an ethanol/water (1:1 by volume) mixture, along with PL spectral blue shifting due to changing of aggregation order. It was also found that the crystalline film showed a blue-shifted absorption spectrum relative to the amorphous film and the shift of the absorption edge of the spectra could match that of corresponding PL spectra. The FT-IR spectrum of crystal powders of **1** displayed more vibration modes compared with that of amorphous powders, suggesting the existence of different π-overlaps or different molecular conformations. The crystals of 1-methyl-1,2,3,4,5-pentaphenylsilole and hexaphenylsilole also showed blue-shifted PL emissions of their amorphous solids, with a comparable PL spectral shift of **1**. Developing of a silole solution on a TLC plate readily brought about an amorphous thin layer. Our results suggest that crystalline films of AIE-active siloles are potential emissive layers for efficient blue OLEDs with stable color and long lifetime.

Introduction

The photoluminescence (PL) quantum yields of conjugated organic emitters normally decrease in the solid state, along with red shifts of PL spectra compared to those in solutions, due to the formation of delocalized excitons or excimers.[1] The aggregation-induced quenching of light emission has been a thorny problem in the development of efficient organic light-emitting diodes (OLEDs) because the organic emitters are normally used as thin solid films in devices and aggregation is inherently accompanying the film formation.[2] Higher aggregation extent also normally induces red shift of PL spectra in most organic emitters, and it is well understood that the PL emission of a crystal form of an emitter is red shifted relative to that of its amorphous form.[3] Tris(8-hydroxyquinoline)aluminum (Alq_3) and tris(8-hydroxyquinoline)aluminum (Gaq_3), however, are exceptional cases.[4] Brinkmann et al. reported that the PL emissions of the crystalline polymorphs of Alq_3 and Gaq_3 were blue-shifted to the corresponding amorphous thin solid films.[4a,b] The authors attributed the results to a possibly large distribution of molecular packings in the amorphous films that broadened π-overlaps between facing ligands in the amorphous films.[4a] A small blue shift (6 nm) of PL emission of a crystalline thin solid film of Alq_3 relative to its amorphous film was also reported by Yan and co-workers, and this was attributed to Rayleigh scattering for shorter wavelengths.[4c]

Siloles or silacyclopentadienes are a group of five-membered silacyclics that possess a unique low-lying LUMO level associated with the $\sigma^*-\pi^*$ conjugation arising from the interaction between the σ^* orbitals of two exocyclic σ bonds on the silicon atom and the π^* orbital of the butadiene moiety.[5] Siloles exhibit high electron acceptability[5,6] and have been utilized as electron-transporting and light-emitting layers in the fabrication of electroluminescence (EL) devices.[7,8] The optical properties of a silole could be well tuned by judicious design of substituents on its 2,5- and 1,1-positions.[8i,9,10] Different from most organic emitters, siloles show an unique *aggregation-induced emission* (AIE) phenomenon; for example, a 2,3,4,5-tetraphenylsilole (TPS) is virtually nonemissive in solutions, but its aggregates or films are highly luminescent.[10,11] For typical AIE-active molecules, the PL quantum yield of their aggregates can differ from that of molecularly dissolved species by 2 orders

* To whom correspondence should be addressed. Fax: +8620-8711-0606. E-mail: psjwchen@scut.edu.cn (J.C.), poycao@scut.edu.cn (Y.C.).
† South China University of Technology.
‡ Hong Kong University of Science & Technology.

10.1021/jp051873o CCC: $30.25
Published on Web 08/23/2005

CHART 1

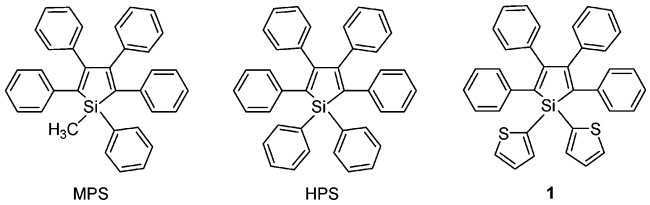

of magnitude. Though a coplanarity hypothesis was proposed for the AIE mechanism of a TPS in the beginning,[11] the hypothesis was not in agreement with the crystal structures of TPSs, which showed that the phenyl peripheries of TPSs were twisted to a great extent (up to 87°) in the solid state.[10] On the basis of further experimental results of enhanced emissions of a TPS solution upon cooling or thickening, we pointed out that the faint emission of a TPS solution was due to rotational deactivations of the phenyl peripheries, and the intense solid-state emission and the cooling- or thickening-enhanced emission of TPS solutions was due to the restrictions of the phenyl rotations.[10] Restricted intramolecular rotation,[10,12] the model for the AIE phenomenon of TPSs and TPS-containing polymers, was soon confirmed by a time-resolved fluorescence technique.[13] Recently we further pointed out that the phenyl rotations of AIE-active molecules could be regarded as rotational relaxations around their equilibrium positions and the magnitude of relaxation time was an important parameter for their fluorescent properties.[14] Thus the AIE-active TPSs showing highly efficient solid-state PL emission are promising light-emitting layers for EL devices. An OLED of 1-methyl-1,2,3,4,5-pentaphenylsilole (MPS, Chart 1) exhibited excellent EL performance, whose maximum current and power efficiencies were 20 cd/A and 14 lm/W, respectively.[15] The maximum external quantum efficiency (η_{EL}) of the EL device was 8%,[15] approaching the limit possible.[16,17] A high η_{EL} of 7% and a very bright light up to 55 880 cd/m^2 at 16 V were reported for hexaphenylsilole (HPS, Chart 1).[18]

AIE-active molecules are normally highly emissive in their crystalline forms; therefore, they are potential candidates for OLEDs, based on the crystalline emissive layer, and for the realization of electrically pumped lasers,[19] since crystals of conjugated molecules possess higher carrier mobility to afford the high current injection, compared to amorphous form.[20] For these purposes, it is necessary to know how to prepare homogeneous crystalline thin solid films and to discover the characteristics of crystalline emissions of AIE-active molecules. In this work, we report a new PL phenomenon of a TPS in the aggregation state. Both blue and green lights could be emitted efficiently by a single emitter, 1,1-bis(2′-thienyl)-2,3,4,5-tetraphenylsilole (**1**, Chart 1), in the solid state. The blue and green emissions corresponded to the crystalline and amorphous states, respectively. Variable PL emissions were found for as-deposited amorphous thin solid films upon treatment in alcohol vapors as well as poor ordered aggregates in liquid media upon aging. A transparent polycrystalline film was achieved via the treatment process. The crystals of MPS and HPS also showed different PL emissions to their amorphous solids, with a comparable PL spectral shift of **1**. The possible origin for the PL phenomenon was discussed.

Experimental Section

General. The ^{1}H and ^{13}C NMR spectra were obtained on a Bruker DRX 400 spectrometer. The UV−visible absorption spectra were recorded on a HP 8453. All the photoluminescence (PL) spectra were performed on a Jobin Yvon Fluorolog-3. GC−mass spectrometry was carried out on a Finnigan Trace 2000. Powder X-ray diffraction was recorded on a Rigaku D/max-IIIA with Cu Kα radiation ($\lambda = 1.54$ Å). Transmission electron microscope (TEM) studies were carried out on a JEOL-2010 under an accelerating voltage of 200 kV. FT-IR spectra were collected on a Bruker Vector 33 with a resolution of 0.3 cm^{-1}. The absolute PL quantum yield of a thin solid film was measured in an integrating sphere (IS-080, Labsphere) under excitation from the 325 nm line of a HeCd laser. Melting point was measured on a Beijing Taike Instruments model X-4. Thin solid films (80 nm) were prepared by vapor deposition under high vacuum on substrates at room temperature. All the reagents were purchased from Aldrich and used without further purification. Tetrahydrofuran (THF) was predried over 4-Å molecular sieves and was distilled from sodium benzophenone ketyl immediately prior to use. MPS and HPS were prepared according to the literature.[21]

The aggregate mixtures of **1** were freshly prepared by adding poor solvents into the silole solutions with vigorous shaking. For example, a nanoparticle mixture of **1** was prepared by adding 8 mL of water to 2 mL of an acetone solution in a 10 mL volumetric flask. The concentrations of all the aggregate mixtures were adjusted to 10 μM unless otherwise specified.

Treatment of the as-deposited thin solid films of **1** was carried out in a sealed container having suitable amount of ethanol or ethanol/water (1:1 by volume) mixture at ambient temperature.

The X-ray diffraction intensity data were collected at 100 K on a Bruker-Nonius Smart Apex CCD diffractometer with graphite-monochromated Mo−Kα radiation. The single crystal of **1** was grown from toluene/heptane mixture. Processing of the intensity data was carried out using the SAINT and SADABS routines, and the structure solution and refinement were done by the SHELXTL suite of X-ray programs (version 6.10).

Synthesis of 1,1-Bis(2′-thienyl)-2,3,4,5-tetraphenylsilole (1). Under dry nitrogen, 180 mg (25.5 mmol) of freshly cut lithium shavings was added to a solution of diphenylacetylene (5 g, 28.1 mmol) in 20 mL of THF. The mixture was stirred for 12 h at room temperature, which readily afforded 1,4-dilithio-1,2,3,4-tetraphenyl-1,3-butadiene, an intermediate. The resultant THF solution of the intermediate was added dropwise to a solution of silicon(IV) chloride (1.22 mL, 10.7 mmol) in 100 mL of THF. The mixture was stirred for 2 h at room temperature and then refluxed for 5 h, which afforded 1,1-dichloro-2,3,4,5-tetraphenylsilole. After the mixture was cooled to room temperature, 21.4 mL of a 1 M THF solution of 2-thienyllithium (21.4 mmol) was added. The mixture was stirred for 2 h at room temperature and then at 50 °C for 24 h. The mixture was filtered and the crude product was purified on a silica gel column using hexane/chloroform mixture (4:1 by volume) as eluent. Product **1** (3.5 g) was isolated in 60% yield (based on silicon(IV) chloride). Recrystallization from toluene/heptane mixture twice gave 3.0 g of pure compound as yellow-greenish thin sheetlike square crystals. Mp: 223−225 °C. FT-IR (KBr), υ (cm^{-1}): 3098, 3055, 3022, 1948, 1876, 1816, 1749, 1652, 1595, 1571, 1531, 1483, 1441, 1399, 1326, 1298, 1211, 1085, 1074, 1026, 1001, 987, 935, 916, 852, 839, 789, 761, 745, 722, 713, 697, 663, 650, 609, 572, 526, 509, 482, 449, 408. ^{1}H NMR (400 MHz, $CDCl_3$), δ (ppm): 7.74 (d, 2H), 7.52 (d, 2H), 7.25 (dd, 2H), 7.05 (m, 12H), 6.97 (m, 4H), 6.89 (m, 4H). ^{13}C NMR (100 MHz, $CDCl_3$), δ (ppm): 156.8, 139.2, 139.1, 138.9, 133.5, 130.3, 130.1, 129.88, 129.86, 129.0, 128.2, 127.9, 127.0, 126.3.

SCHEME 1

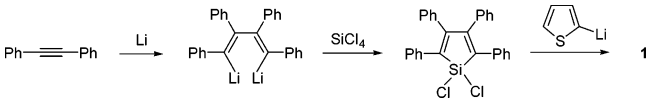

MS: *m*/*z* 550 (M^+). UV ($CHCl_3$) λ_{max} (nm)/ϵ_{max} (dm^3 mol^{-1} cm^{-1}): 245/4.13 × 10^4, 372/8.84 × 10^3.

Results

Synthesis and Single-Crystal Structure. Siloles bearing a thiophene moiety at the 2,5-positions were reported by Tamao et al.[8i] In this study, compound **1**, a novel silole with thiophene lingkages to the silicon atom, was prepared by the reaction of 1,1-dichloro-2,3,4,5-tetraphenylsilole with 2-thienyllithium (Scheme 1). We first synthesized 1,4-dilithio-1,2,3,4-tetraphenyl-1,3-butadiene according to a modified Curtis method: lithium shavings reacted with an excess of diphenylacetylene so as to avoid side reactions.[10] Then 1,1-dichloro-2,3,4,5-tetraphenylsilole was prepared by the cyclization reaction of the 1,4-dilithio-1,2,3,4-tetraphenyl-1,3-butadiene with silicon(IV) chloride. The dichlorosilole was used in situ and reacted with 2-thienyllithium to afford **1** in a good yield of 60% based on the amount of silicon(IV) chloride. Thin, sheetlike crystals were obtained by recrystallization twice from toluene/heptane mixtures in high yields.

A suitable specimen for crystallography was mounted in air on glass fibers, and its X-ray diffraction intensity data were collected on a diffractometer. The ORTEP drawing of **1** is shown in Figure 1, and its crystal data and analysis parameters are summarized in Table 1. Silole **1** crystallized in the monoclinic system space group $P2_1$. Some of the thiophene rings showed rotational disorder[22] in the unit cell, resulting in somewhat higher values of R1 and wR2. The geometric parameters of the silole are similar to that of formerly reported TPSs with excellent general agreement in their bond lengths and bond angles, and the silole also holds a planar silole core and six twisted aromatic substituents (see Supporting Information for details).[10,23]

Variable PL Emission of Aggregates of 1 Formed in Solutions. Since **1** is a congener of TPS, we postulate that **1** should show AIE activity.[10] The on−off phenomenon of AIE-active molecules was observed (Figure 2A) when water, a nonsolvent of **1**, was added to its acetone solution (the final concentrations being kept unchanged at 10 μM unless otherwise specified). The maximum change of PL intensity of about 200 times is comparable to that of reported TPSs.[10] The trajectory of the peak intensity change suggests that the silole molecules started to aggregate at a water fraction of >50% and the emissive species continued to increase as the water fraction was increased.[10,14] The results indicated that **1** showed the same AIE property as other TPSs and the on−off phenomenon should be explained by restricted intramolecular rotation.[10,14] PL spectra for the intense emissions at water fractions ranging from 60 and 90% are shown in Figure 2B. Aggregates in the mixtures with water fractions of 70−90% (aggregates 70−90), emitted blue-greenish light that peaked at 500 nm. Unexpectedly, however, aggregates 60 emitted a blue light that peaked at 474 nm.

The maximum of the absorption (λ_{ab}) of **1** in chloroform was at 372 nm. Small deviations (within 3 nm) of UV absorptions of **1** in solvents with different polarity, such as cyclohexane, ethyl acetate, and acetonitrile, demonstrated that **1** is not a solvatochromic molecule.[24]

For the freshly prepared aggregates 60−90, all the mixtures were macroscopically homogeneous with no precipitate. The

TABLE 1: Summary of Crystal Data and Intensity Collection Parameters for Silole 1

empirical formula	$C_{36}H_{26}S_2Si$
mol wt	550.78
crystal dimensions, mm	0.40 × 0.35 × 0.1
crystal system	monoclinic
space group	$P2_1$
unit cell constants	
a, Å	9.878(2)
b, Å	9.840(2)
c, Å	29.591(6)
α, deg	90.00
β, deg	90.29(3)
γ, deg	90.00
V, Å^3	2876.2(10)
Z	4
$D_{calcd.}$, g cm^{-3}	1.272
F_{000}	1152
temp, K	100(2)
radiation (*λ*), Å	Mo Kα, 0.710 70
μ(Mo Kα) mm^{-1}	0.110
$2\theta_{max}$, deg (completeness)	50 (98.6%)
no. of collected reflns	9822
no. of unique reflns	8282
data/restraints/parameters	8282/1/673
R_1, wR_2 [obs $I > 2\sigma(I)$]	0.1267, 0.2861
R_1, wR_2 (all data)	0.1434, 0.2920
goodness of fit, *S*	1.663
residual peak/hole e^- Å^{-3}	0.725/−0.662
transmission ratio	1.00/0.76

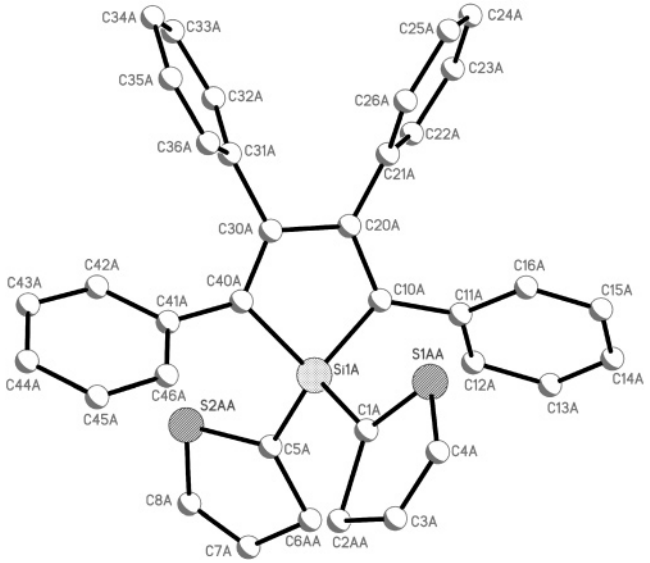

Figure 1. ORTEP drawing of **1**; the hydrogen atoms were omitted for clarity.

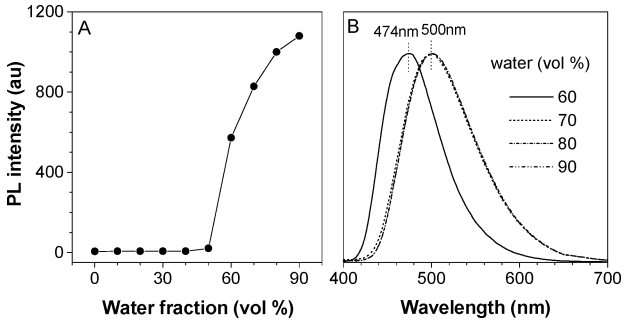

Figure 2. (A) PL intensity of **1** vs composition of the water/acetone mixture. (B) Normalized PL spectra of **1** in the mixtures with water fraction ranging between 60 and 90%. Concentration of **1**, 10 μM; excitation wavelength, 372 nm.

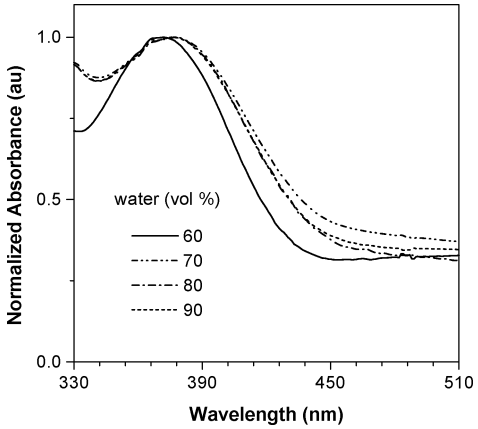

Figure 3. Normalized UV absorption spectra of **1** in water/acetone mixtures with different volume fractions of water; concentration of **1**, 10 μM.

λ_{ab} values for aggregates 70−90 were all at 378 nm, while the λ_{ab} for the aggregates 60 was at 372 nm (Figure 3). The 6-nm blue shift of absorption between aggregates 60 and aggregates 70−90 was much lower than the corresponding blue shift of PL spectra. The absorbance in the longer wavelengths for all the aggregates was due to light scattering of the aggregates, which effectively decreased the light transmission through the silole mixtures. Similar results were also reported previously.[10]

However, the aggregates in water/acetone mixtures were not stable suspensions; the mixtures of aggregates 60 and aggregates 70 became obviously turbid in 20 min, but the mixtures of aggregates 80 and aggregates 90 remained macroscopically homogeneous during such a storage time. The mixtures of aggregates 60 and aggregates 90 were dropped on glassy carbon films supported by copper grids. After full drying in a vacuum oven, the samples were analyzed on a transmission electron microscope (TEM). Their TEM images are shown in Figure 4A,C. The image for aggregates 60 (Figure 4A) indicated that aggregates 60 were square sheets such as the bulk crystals, obtained by recrystallization from a toluene/heptane mixture. The dimensions of the square sheets were about 3.3 μm × 3.3 μm, demonstrating that the aggregates 60 were not of nano-dimension upon aging. The selected-area electron diffraction (SAED) of the square sheets indicated that they were single crystals (Figure 4B). We also carried out SAED of the bulk crystals for comparison (not shown). It was found that the SAED pattern of aggregates 60 was consistent with that of bulk crystals. Therefore, the single crystals of aggregates 60 should possess the same structure as the bulk crystals, indicating that the different solvent systems did not alter the crystallization form of the silole. Aggregates 90, however, were irregular particles (Figure 4C), and the SAED image showed rather weak diffraction rings (Figure 4D), indicating that the degree of order of aggregates 90 is largely lower than that of aggregates 60. The results demonstrated that the different PL emissions of aggregates 60−90 in Figure 2B were probably due to different aggregation order. The aggregation order of the silole particles formed in the water/acetone mixtures was determined by the volume fraction of the nonsolvent (water). At a water fraction of 60%, which was only slightly higher than the critical aggregation point (50%), the silole molecules could pack into well-ordered crystals. But at higher nonsolvent fractions (70−90%), poorly ordered packing took place.

The maximum of PL spectrum (λ_{em}) of the aggregates 60 in the mixture remained at 474 nm upon aging, demonstrating that the crystalline form is a stable phase of **1**, but the emissions of

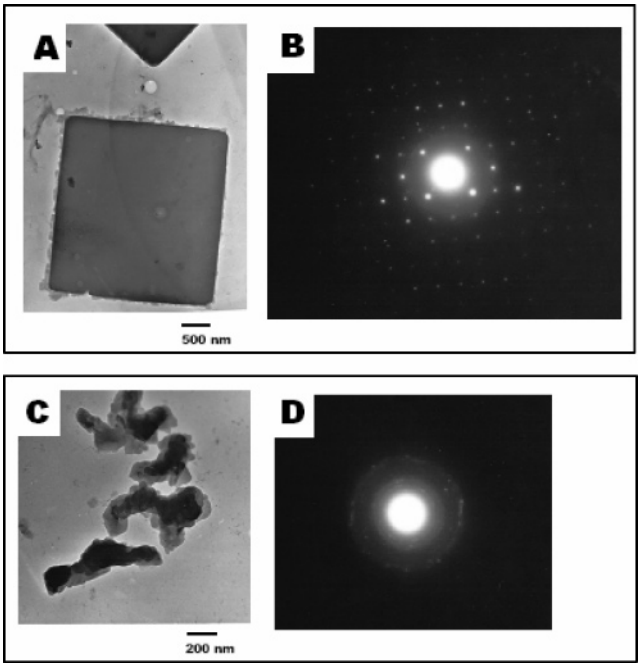

Figure 4. TEM images of aggregates of **1** prepared by dropping its water/acetone (A) 6:4 or (C) 9:1 (by volume) mixture on glassy carbon film and then fully drying the sample under vacuum. Selected-area electron diffraction patterns B and D correspond to images A and C, respectively.

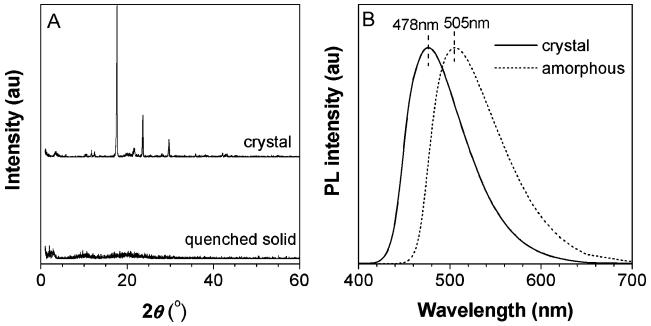

Figure 5. (A) Powder X-ray diffraction patterns of bulk crystals of **1** and its amorphous solid prepared by quenching its melt with liquid nitrogen. (B) PL spectra of the silole crystals and its amorphous solid; excitation wavelength, 372 nm.

the poorly ordered aggregates 70−90 showed blue-shift toward the λ_{em} of the crystalline emission during the aging (See Supporting Information for details). The experimental results also suggested that PL particle size effect[26] did not contribute to the PL emission of **1** (See Supporting Information for details).

The big reliance of the PL emission of **1** on the aggregation order is unusual, since higher aggregation extent normally induces red-shift of PL spectra for most organic emitters due to the formation of delocalized excitons.[1,3]

Variable PL Emission of Macroscopically Dry Solids of 1. To pursue the aggregation-order-dependent PL emission of the silole particles in the water/acetone mixtures, we characterized the PL spectra of macroscopically dry solids of **1** in different aggregation states. The powder X-ray diffraction profiles showed that the bulk crystals were highly ordered,[25] while the amorphous solid of **1** was successfully prepared by quenching its melt with liquid nitrogen (Figure 5A). Upon excitation, the crystals emitted a blue light that peaked at 478 nm, while the amorphous solid emitted a green light that peaked at 505 nm (Figure 5B). The results indicated that both blue and green lights could be obtained by judicious control of the

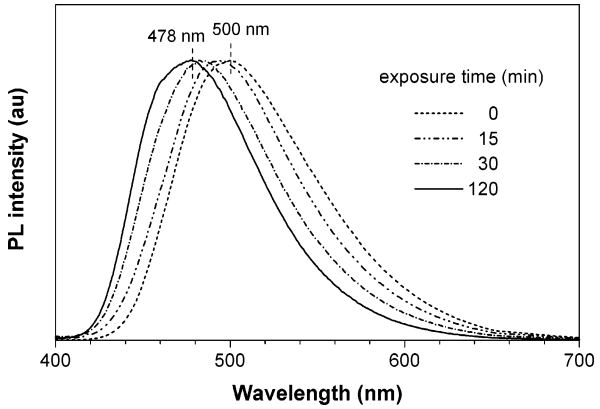

Figure 6. PL spectral shifting of thin solid films (80 nm) of **1** deposited on glass substrate when treated by the vapor of an ethanol/water (1:1 by volume) mixture at 20 °C for different exposure time; excitation wavelength, 372 nm.

aggregation morphology of **1**. The PL spectra of **1** shifted as a whole from longer wavelengths to shorter wavelengths suggest that Rayleigh scattering is not dominant for the largely blue-shifted PL spectra of the silole crystals.[4c] The shift of PL spectra was practically identical to that between aggregates 60 and aggregates 70−90, from which the PL spectral reliance on aggregation order of **1** was doubly confirmed. It was also found that changing of the excitation wavelength between 325 and 400 nm did not alter the peak positions of the PL spectra of the crystals and the amorphous solid.

Variable PL Emission of Thin Solid Film of 1 Treated by Alcohol Vapors. In addition to the variation of PL spectra of **1** in liquid media of nonsolvent/solvent mixtures, PL spectra of its thin solid film (80 nm) on glass substrate also showed similar shift upon treatment in alcohol vapors. The as-deposited film on glass was transparent and its λ_{em} peaked at 500 nm, close to that of the amorphous solid in the dry state. It became opaque after the film was exposed to the vapor of ethanol at 20 °C for 1 h. The dried opaque film[27] emitted at 478 nm, identical to the emission of crystals of **1** in the dry state. The transformation from the initially transparent film to the opaque film is a signature of inhomogeneous crystallization. Instead of ethanol, with an ethanol/water (1:1 by volume) mixture, the film kept transparent after a treatment for 2 h. The PL spectral blue shifting during the treatment is shown in Figure 6. After treatment for 15 min, the film emitted at 494 nm. The λ_{em} further blue-shifted to 484 nm after a longer treatment (30 min). After treatment for 120 min, the λ_{em} of the film was at 478 nm, also identical to that of crystals in the dry state. After further increase of treatment time to 3 h, the λ_{em} remained at 478 nm.

Electron diffraction was performed on the TEM for thin solid films deposited on glassy carbon films. It was found that the as-deposited film was amorphous. But the film treated by the vapor of the ethanol/water (1:1 by volume) mixture at 20 °C for 2 h displayed an intense crystalline diffraction pattern (see Figure 7). Thus, the PL spectral blue-shifting of the film treated by the solvent vapor should result from crystallization of the film. The solvent vapor mediated crystallization may be attributed to the noncoplanar and dendritic structure of **1** that retains voids big enough for solvent vapor molecules to enter. Since the diffraction pattern is quite different from that of the crystals formed in solutions (see Figure 4B), silole **1** might form a new thin-film polymorph during the treatment. The polymorph still needs further confirmation. The absolute PL quantum yield for the as-deposited amorphous film, measured in an integrating sphere, was 0.98, close to unity. A similar result was reported

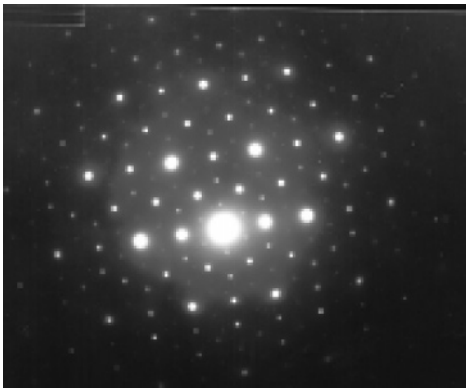

Figure 7. Selected-area electron diffraction pattern of the thin solid film treated by the vapor of an ethanol/water (1:1 by volume) mixture at 20 °C for 2 h.

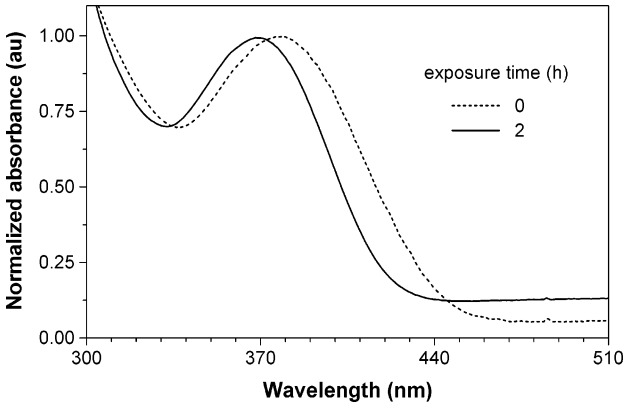

Figure 8. UV absorption spectra of thin solid films of **1** before and after the treatment by the vapor of an ethanol/water (1:1 by volume) mixture at 20 °C for 2 h.

previously for the thin solid film of a TPS derivative.[8e] The treated crystalline film also possessed a high absolute PL quantum yield of 0.80. The high PL efficiency of **1** in the crystalline state should be attributed to the AIE characterization of TPSs. The results indicated that both blue and green lights could be emitted efficiently by **1**. Our results also open a space for the device engineering in full color display.

Figure 8 shows the absorption spectra of the thin solid films of **1** before and after the treatment. The absorption peak of the amorphous film associated with the silole ring was at 379 nm, while that of the crystalline film was at 369 nm. The absorption edges of the spectra showed a bigger difference. The absorption edges of the amorphous film and the crystalline film were at 447 and 425 nm, respectively. The absorption edge of the crystalline film blue-shifted 22 nm relative to that of the amorphous film, which matched the shift of the corresponding PL spectra, as shown in Figure 6. It is well-known that the absorption edge affects the PL spectra more directly for light-emitting materials, compared with the absorption peak. However, comparable absorption edge difference was not observed for the aggregates in liquid media of solvent/nonsolvent mixtures (see Figure 3), this could be attributed to the disturbance of the strong light scattering of the aggregates.

PL Spectral Reliance on Aggregation Order of MPS and HPS. We further checked the PL emissions of the crystals and amorphous powders of MPS and HPS, two derivatives of TPSs. MPS and HPS were prepared according to the published literature,[21] and both of the two siloles could crystallize in a triclinic system space group $P\bar{1}$.[28] The crystals of the two siloles studied here were grown from a toluene/heptane mixture. The

TABLE 2: Emission Characteristics of 1, MPS, and HPS[a]

		λ_{em} (nm)			
silole	space group	crystal[c] powder	amorphous powder[d]	thin layer[e]	$\Delta\lambda_{em}$ (nm)[e]
1	$P2_1$	478	505	500	27
MPS	$P\bar{1}$[b]	462	490	490	28
HPS	$P\bar{1}$[b]	470	495	495	25

[a] Excitation wavelength 372 nm. [b] See ref 28. [c] Recrystallization from a toluene/heptane mixture. [d] Prepared by quenching from the melt state by liquid nitrogen. [e] Absorbed on a TLC plate prepared by developing with a chloroform solution of a silole (2 mg/mL). [f] Calculated by the λ_{em} of amorphous powder minus that of crystal powder.

amorphous powders of the two siloles were prepared by quenching from the melt state by liquid nitrogen. The PL results are listed in Table 2 with corresponding data of **1** for comparison. The λ_{em} values of the crystals and the amorphous powders of MPS were at 462 and 490 nm, respectively. The emission of the crystals blue-shifted 28 nm relative to that of the amorphous powders, becoming almost identical to that of **1**. The powder X-ray diffraction showed that the crystals of MPS were polycrystalline (see Supporting Information). That the PL emission of MPS relied on the aggregation order gave a new explanation to the PL spectral shift in MPS/polymer blends.[11] Similar PL spectral reliance on aggregation order was also found for HPS: 470 nm for its crystals and 495 nm for its amorphous solids. Our results suggest that the PL spectral shift on aggregation order might be a characteristic of TPSs.

We have reported a TLC-based method to measure the solid-state luminescence spectra that could be applicable to thermally unstable and difficult-to-melt organic and organometallic compounds.[10] Thin layers of **1**, MPS, and HPS were absorbed on TLC plates by developing with their chloroform solutions. Their emission maxima are also listed in Table 2. The λ_{em} for **1** was at 500 nm, close to that of its amorphous emission. The λ_{em} values for MPS and HPS were at 490 and 495 nm, completely identical to that of the corresponding amorphous emissions. The random packing of the silole molecules should be attributed to the adsorption of the silica to the molecules.

The different PL emissions as shown in Figure 2B and the variable PL emissions of aggregates 70−90 in water/acetone mixtures upon aging were not found for MPS and HPS, probably because the aggregate formation in a nonsolvent/solvent mixture was a rapid process and the formation of crystalline aggregates in the mixture should strongly rely on the chemical structure of a silole. MPS and HPS readily formed amorphous aggregates in water/acetone mixtures at any water fractions based on their emission spectra. That is why the phenomenon of PL spectral reliance on aggregation order of TPSs as reported here remained unknown for a long time.

Discussions

Similar blue-shifted PL emission of the crystal compared to the amorphous solid was also reported for Alq_3 and Gaq_3 by Brinkmann et al.[4a,b] The Alq_3, Gaq_3, and TPSs are organometallic compounds. Compared with Alq_3 or Gaq_3, a TPS molecule also shows some similarity in the molecular configuration. For a TPS molecule, the four phenyl peripheries are quite twisted out of the plane of the central silole core, and aromatic substituents on the silicon atom are also twisted due to the sp^3 hybridization of the silicon atom.[10] The three 8-hydroxyquinoline ligands of an Alq_3 molecule are also arranged twisted out.[4a] The geometric structures of an Alq_3 molecule and a TPS molecule are thus quite different from the coplanar structure of fluorenic-core molecules, whose crystals showed red-shifted PL emission of their amorphous form, as reported by Destri et al.[3] It was found that polymorphism could greatly affect the PL emissions of Alq_3 and Gaq_3.[4a,b] On the basis of our experimental results, there is no direct evidence that the crystalline polymorphism has large influence on the PL spectra of a TPS.

Brinkmann et al. pointed out that the possible origin for the unusual PL spectral shift of Alq_3 might be due to broadened π overlaps between facing ligands in the amorphous state.[4a] The PL spectral reliance on the aggregation order of **1** observed here may also have a similar origin. Due to the twisted arrangements of the peripheral aromatic rings of **1**, the distance between two adjacently chromophoric silole cores is far from the normal $\pi-\pi$ interaction distance (ca. 3−4 Å). The unique structure may play important roles in suppressing excimer formation and closing nonradiative pathways in the aggregation state.[14] But $\pi-\pi$ overlaps can occur between the silole molecules. A schematic graph is given in Figure 9 to show intermolecular short contacts of **1**.[29] The peripheral aromatic rings can establish many short contacts in the crystal structure. In amorphous aggregates, the intermolecular short contacts might be changed. The different extents of the short contacts should result in different molecular

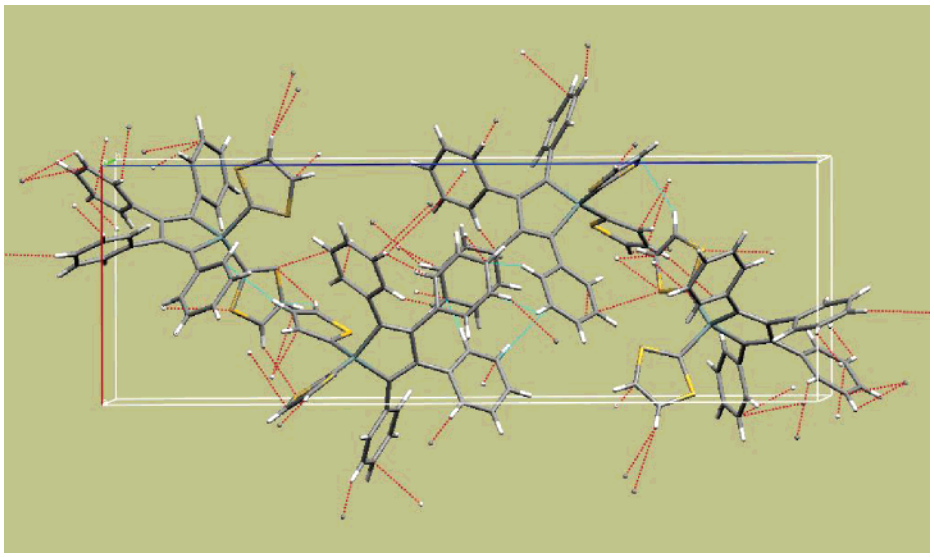

Figure 9. A schematic graph of intermolecular short contacts (red and cyan lines) of **1** in a unit cell as viewed along the *b* axis.[29]

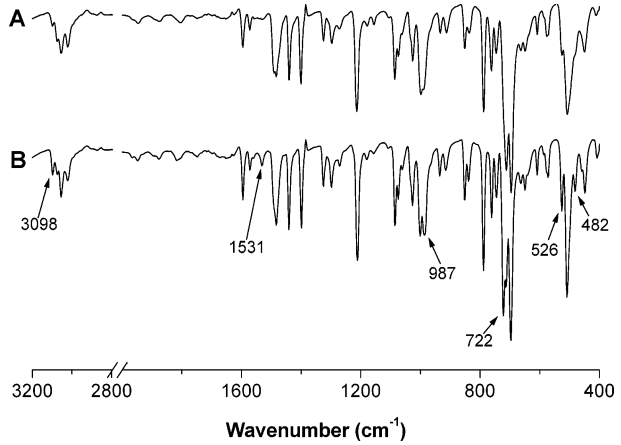

Figure 10. FT-IR spectra of **1** dispersed in a KBr pellet: (A) amorphous powders prepared by quenching from the melt state by liquid nitrogen and (B) crystal powders prepared by recrystallization from toluene/heptane mixture. The axis is broken arbitrarily from 2000 to 2800 cm^{-1} for clarity.

conformations for **1** in the crystalline state and in the amorphous state,[30] and this was confirmed by FT-IR spectra. The FT-IR spectra of the amorphous powder and crystal powder of **1** are shown in Figure 10. The FT-IR spectrum of the crystal exhibited remarkable differences from that of the amorphous powders. All peaks displayed in the FT-IR spectrum of the amorphous powders still remained in the spectrum of the crystal powders. But for the crystal powders, some new and enhanced peaks could be found at 3098, 1531, 987, 722, 526, and 482 cm^{-1}. The enhanced peak at 3098 cm^{-1} should be due to the C−H stretching mode of the benzene rings and/or thiophene rings.[31] The new peak at 1531 cm^{-1} is located in the bands of skeleton vibrations of a thiophene ring.[31] Comparable infrared absorptions had been assigned to a 2-thienyl group.[32] The new peak at 987 cm^{-1} is mainly due to the in-plane C−H bending mode of the benzene rings.[31] The new peak at 722 cm^{-1} should be due to the out-of-plane C−H bending mode of the benzene rings and/or thiophene rings.[31,33] The different FT-IR spectra might be a method to differentiate the aggregation order of **1**. We have found that the absorption edge of the crystalline film blue-shifted 22 nm relative to that of the amorphous film, which matched the shift of the corresponding PL spectra. Thus the crystalline and amorphous forms of **1** should possess different electron transition levels due to different transition dipoles, resulting from the different intermolecular short contacts or different molecular conformations.[34]

Conclusions

We synthesized 1,1-bis(2′-thienyl)-2,3,4,5-tetraphenylsilole in good yield by using a modified Curtis procedure. The PL emission of the silole showed unusual reliance on its aggregation order: crystalline aggregates emitted a blue light while amorphous ones emitted a green light. Variable PL emissions were observed for the poorly ordered aggregates in the water/acetone mixtures as well as the amorphous film in the atmosphere of alcohols. The aggregates in the mixtures and the films could finally exhibit blue light emissions of the crystals. Compared with the amorphous film, the crystalline film showed blue-shifted absorption spectra, and the blue shift of the absorption edge of the spectra could match that of corresponding PL spectra. But such absorption difference due to different aggregation orders was not found for aggregates in the mixtures, probably due to the disturbance of light scattering of the aggregates. The crystals of MPS and HPS also showed different PL emissions for their amorphous solids, with comparable PL spectral shift. The thin layers of **1**, MPS, and HPS, absorbed on TLC plates, showed amorphous PL emissions. The FT-IR spectrum of crystal powders of **1** exhibited more vibrations compared with that of amorphous powders, suggesting the existence of different π overlaps or different molecular conformations.

Treatment of the as-deposited amorphous film of **1** by the vapor of a ethanol/water (1:1 by volume) mixture is a method to obtain a transparent crystalline film. Both of the crystalline film and the amorphous film possess high absolute PL quantum yields. Our results suggest that crystalline films of AIE-active siloles are potential emissive layers for efficient blue-light OLEDs with stable color and long lifetime.

Acknowledgment. Financial support from Natural Science Foundation of China (Grant 50303006), Special Funds for Major State Basic Research Projects (Grant 2002CB613404), and Education Ministry of China (Program for NCET and SRF for ROCS) is gratefully acknowledged.

Supporting Information Available: Detailed description, PL spectra, and UV spectra of the aggregates 50−90 of **1** at different concentrations of water/acetone mixtures upon aging; powder X-ray diffraction pattern of crystals of MPS; CIF format file and crystal structure with atom labels, tables of crystal data, structure solution and refinement, atomic coordinates, bond lengths and angles, and anisotropic displacement parameters for **1**. This material is available free of charge via the Internet at http://pubs.acs.org.

References and Notes

(1) (a) Jenekhe, S. A.; Osaheni, J. A. *Science* **1994**, *265*, 765. (b) Friend, R. H.; Gymer, R. W.; Holmes, A. B.; Burroughes, J. H.; Marks, R. N.; Taliani, C.; Bradley, D. D. C.; Dos Santos, D. A.; Bredas, J. L.; Logdlund, M.; Salaneck, W. R. *Nature* **1999**, *397*, 121. (c) Deans, R.; Kim, J.; Machacek, M. R.; Swager, T. M. *J. Am. Chem. Soc.* **2000**, *122*, 8565.

(2) *Film Formation in Coatings: Mechanisms, Properties, and Morphology*; Provder, T., Urban, M. W., Eds.; American Chemical Society: Washington, DC, 2001.

(3) Destri, S.; Pasini, M.; Botta, C.; Porzio, W., Bertini, F.; Marchio, L. *J. Mater. Chem.* **2002**, *12*, 924 and references therein.

(4) (a) Brinkmann, M.; Gadret, G.; Muccini, M.; Taliani, C.; Masciocchi, N.; Sironi, A. *J. Am. Chem. Soc.* **2000**, *122*, 5147. (b) Brinkmann, M.; Fite, B.; Pratontep, S.; Chaumont C. *Chem. Mater.* **2004**, *16*, 4267. (c) Qin, D. S.; Li, D. C.; Wang, Y.; Zhang, J. D.; Xie, Z. Y.; Wang, G.; Wang, L. X.; Yan, D. H. *Appl. Phys. Lett.* **2000**, *78*, 437.

(5) For reviews, see: (a) Hissler, M.; Dyer, P. W.; Reau, R. *Coord. Chem. Rev.* **2003**, *244*, 1. (b) Sadimenko, A. P. *Adv. Heterocycl. Chem.* **2001**, *79*, 115. (c) Lee, V. Y.; Sekiguchi, A.; Ichinohe, M.; Fukaya, N. *J. Organomet. Chem.* **2000**, *611*, 228. (d) Hermanns, J.; Schmidt. B. *J. Chem. Soc., Perkin Trans. 1* **1999**, 81. (e) Yamaguchi, S.; Tamao, K. *J. Chem. Soc., Dalton Trans.* **1998**, 3693. (f) Dubac, J.; Guerin, C.; Meunier, P. In *The Chemistry of Organic Silicon Compounds*; Rappoport, Z., Apeloig, Y, Eds.; Wiley: New York, 1998; Vol. 2, Chapter 34. (g) Yamaguchi, S.; Tamao, K. *Bull. Chem. Soc. Jpn.* **1996**, *69*, 2327. (h) Wrackmeyer, B, *Coord. Chem. Rev.* **1995**, *145*, 125. (i) Chuit, C.; Corriu, R. J. P.; Reye, C.; Young, J. C. *Chem. Rev.* **1993**, *93*, 1371. (j) Colomer, E.; Corriu, R. J. P.; Lehureux, M. *Chem. Rev.* **1990**, *90*, 265.

(6) Among conjugated five-membered heterocyclics (pyrrole, thiophene, furan, etc.), siloles have the highest electron-accepting ability.[5]

(7) (a) Tamao, K.; Uchida, M.; Izumizawa, T.; Furukawa, K.; Yamaguchi, S. *J. Am. Chem. Soc.* **1996**, *118*, 11974. (b) Murata, H.; Malliaras, G. G.; Uchida, M.; Shen, Y.; Kafafi, Z. H. *Chem. Phys. Lett.* **2001**, *339*, 161.

(8) (a) Yu, G.; Yin, S.; Liu, Y.; Chen, J.; Xu, X.; Sun, X.; Ma, D.; Zhan, X.; Peng, Q.; Shuai, Z.; Tang, B.; Zhu, D.; Fang, W.; Luo, Y. *J. Am. Chem. Soc.* **2005**, *127*, 6335. (b) Lee, J.; Liu, Q. D.; Motala, M.; Dane, J.; Gao, J.; Kang, Y.; Wang, S. *Chem. Mater.* **2004**, *16*, 1869. (c) Lee, J.; Liu, Q. D.; Bai, D. R.; Kang, Y.; Tao, Y.; Wang, S. *Organometallics* **2004**, *23*, 6205. (d) Chen, H.; Chen, J.; Qiu, C.; Tang, B. Z.; Wong, H.; Kwok, H. S. *IEEE J. Select. Topics Quantum Electron.* **2004**, *10*, 10. (e) Murata; H.;

Kafafi; Z. H.; Uchida; M. *Appl. Phys. Lett*. **2002**, *80*, 189. (f) Uchida, M.; Izumizawa, T.; Nakano, T.; Yamaguchi, S.; Tamao, K.; Furukawa, K. *Chem. Mater*. **2001**, *13*, 2680. (g) Ohshita, J.; Kai, H.; Takata, A.; Iida, T.; Kunai, A.; Ohta, N.; Komaguchi, K.; Shiotani, M.; Adachi, A.; Sakamaki, K.; Okita, K. *Organometallics* **2001**, *20*, 4800. (h) Hay, C.; Hissler, M.; Fischmeister, C.; Rault-Berthelot, J.; Toupet, L.; Nyulaszi, L.; Reau, R. *Chem. Eur. J.* **2001**, *7*, 4222. (i) Yamaguchi, S.; Endo, T.; Uchida, M.; Izumizawa, T.; Furukawa, K.; Tamao, K. *Chem. Eur. J*. **2000**, *6*, 1683. (j) Wang, F.; Luo, J.; Yang, K.; Chen, J.; Huang, F.; Cao, Y. *Macromolecules* **2005**, *38*, 2253.

(9) (a) Boydston, A. J.; Yin, Y.; Pagenkopf, B. L. *J. Am. Chem. Soc.* **2004**, *126*, 10350. (b) Boydston, A. J.; Yin, Y.; Pagenkopf, B. L. *J. Am. Chem. Soc*. **2004**, *126*, 3724. (c) Boydston, A. J.; Pagenkopf, B. L. *Angew. Chem., Int. Ed.* **2004**, *43*, 6336. (d) Roques, N.; Gerbier, P.; Nakajima, S.; Teki, Y.; Guerin, C. *J. Phys. Chem. Solids*, **2004**, *65*, 759. (e) Ohshita, J.; Lee, K. H.; Kimura, K.; Kunai, A. *Organometallics* **2004**, *23*, 5622. (f) Tracy, H. J.; Mullin, J. L.; Klooster, W. T.; Martin, J. A.; Haug, J.; Wallace, S.; Rudloe, I.; Watts, K. *Inorg. Chem.* **2005**, *44*, 2003. (g) Li, Z.; Dong, Y.; Mi, B.; Tang, Y.; Haussler, M.; Tong, H.; Dong, Y.; Lam, J. W. Y.; Ren, Y.; Sung, H. H. Y.; Wong, K. S.; Gao, P.; Williams, I. D.; Kwok, H. S.; Tang, B. Z. *J. Phys. Chem. B* **2005**, *109*, 10061.

(10) Chen, J.; Law, C. C. W.; Lam, J. W. Y.; Dong, Y.; Lo, S. M. F.; Williams, I. D.; Zhu, D.; Tang, B. Z. *Chem. Mater*. **2003**, *15*, 1535.

(11) Luo, J.; Xie, Z.; Lam, J. W. Y.; Cheng, L.; Chen, H.; Qiu, C.; Kwok, H. S.; Zhan, X.; Liu, Y.; Zhu, D.; Tang, B. Z. *Chem. Commun.* **2001**, 1740.

(12) Chen, J.; Xie, Z.; Lam, J. W. Y.; Law, C. C. W.; Tang, B. Z. *Macromolecules* **2003**, *36*, 1108.

(13) Ren, Y.; Lam, J. W. Y.; Dong, Y.; Tang, B. Z.; Wong, K. S. *J. Phys. Chem. B* **2005**, *109*, 1135.

(14) Chen, J.; Xu, B.; Ouyang, X.; Tang, B. Z.; Cao, Y. *J. Phys. Chem. A* **2004**, *108*, 7522.

(15) Chen, H. Y.; Lam, J. W. Y.; Luo, J. D.; Ho, Y. L.; Tang, B. Z.; Zhu, D. B.; Wong, M.; Kwok, H. S. *Appl. Phys. Lett.* **2002**, *81*, 574.

(16) The highest external quantum efficiency for a singlet emitter has been theoretically predicted to be ~5.5%, but recent research in the area suggests that this limit may be uplifted to ~9%.[17]

(17) (a) Cao, Y.; Parker, I. D.; Yu, G.; Zhang, C.; Heeger, A. J. *Nature* **1999**, *397*, 414. (b) Kim, J. S.; Ho, P. K.; Greenham, N. C.; Friend, R. H. *J. Appl. Phys*. **2000**, *88*, 1073. (c) Shuai, Z.; Beljonne, D.; Silbey, R. J.; Bredas, J. L. *Phys. Rev. Lett.* **2000**, *84*, 131. (d) Wohlgenannt, M.; Tandon, K.; Mazumdar, S.; Ramaesha, S.; Vardeny, Z. V. *Nature* **2001**, *409*, 494.

(18) Chen, H.; Chen, J.; Qiu, C.; Tang, B. Z.; Wong, H.; Kwok, H. S. *Proceedings of the 6th Chinese Optoelectronicis Symposium*; Hong Kong, China, September 12−14, 2003; IEEE: New York; pp 182.

(19) Though Schön et al. claimed that electrically pumped lasers were realized (Schön, J. H.; et al. *Science* **2000**, *289*, 599; *Science* **2000**, *290*, 963), the papers have since been retracted by the journal *(Science* **2002**, *298*, 961).

(20) (a) Funahashi, M.; Hanna, J. *Phys. Rev. Lett.* **1997**, *78*, 2184. (b) Schein, L. B.; McGhie, A. R. *Phys. Rev. B* **1979**, *20*, 1631.

(21) Tang, B. Z.; Zhan, X.; Yu, G.; Lee, P. P. S.; Liu, Y.; Zhu, D. *J. Mater. Chem.* **2001**, *11*, 2874.

(22) (a) Devi, S. S.; Malathi, R.; Rajan, S. S.; Aravind, S.; Krishnakumari, G. N.; Ravikumar, K. *Acta Crystallogr. E*, **2004**, *60*, O117. (b) Barcon, A.; Cote, M. L.; Brunskill, A. P. J.; Thompson, H. W.; Lalancette, R. A. *Acta Crystallogr. C*, **1997**, *53*, 1842.

(23) Chen, J.; Peng, H.; Law, C. C. W.; Dong, Y.; Lam, J. W. Y.; Williams, I. D.; Tang, B. Z. *Macromolecules* **200**3, *36*, 4319.

(24) Many thiophene-containing compounds behaved solvatochromism, see for example: (a) El-Sayed, M.; Muller, H.; Rheinwald, G.; Lang, H.; Spange, S. *Chem. Mater*. **2003**, *15*, 746. (b) Abbotto, A.; Bradamante, S.; Facchetti, A.; Pagani, C. A. *J. Org. Chem.* **1997**, *62*, 5755.

(25) The three peaks for the powder X-ray diffraction of the crystals of **1** were at 2θ values of 17.66, 23.64, and 29.70° with *d*-spacings of 5.018, 3.760, and 3.006 Å, respectively. Their relative intensities were 99, 26, and 11, respectively.

(26) Xiao, D.; Xi, L.; Yang, W.; Fu, H.; Shuai, Z.; Fang, Y.; Yao, J. *J. Am. Chem. Soc.* **2003**, *125*, 6740.

(27) All the fumed films were dried by compressed air before PL characterization, and no PL spectral changing was found by further drying of the films in a vacuum oven for several hours, indicating that the blue shifting of the fumed films was not due to solvent adsorption.

(28) It is difficult to grow single crystals of MPS from toluene/heptane mixture. Recently, single crystal of MPS grown from methanol was successful.[8a] The single crystal structure of HPS was characterized successfully with toluene/heptane grown samples[10] and was further confirmed by a recent report.[9f]

(29) The schematic graph of intermolecular short contacts was exported with the single-crystal CIF file of **1** and Mercury 1.1 (Copyright CCDC, http://www.ccdc.cam.ac.uk/mercury/) with default parameters.

(30) Aleksa, V.; Klaeboe, P.; Nielsen, C. J.; Guirgis, G. A.; Durig, J. R. *J. Raman Spectrosc.* **2004**, *35*, 975.

(31) Pretsch, E.; Buhlmann, P.; Affolter, C. *Structure Determination of Organic Compounds*, Springer-Verlag: Berlin, 2000.

(32) Ruiz Delgado, M. C.; Hernandez, V.; Lopez Navarrete, J. T.; Tanaka, S.; Yamashita, Y. *J. Phys. Chem. B.* **2004**, *108*, 2516.

(33) Casado, J.; Pappenfus, T. M.; Miller, L. L.; Mann, K. R.; Orti, E.; Viruela, P. M.; Pou-Amerigo, R.; Hernandez, V.; Lopez Navarrete, J. T. *J. Am. Chem. Soc.* **2003**, *125*, 2524.

(34) (a) Wright, J. D. *Molecular Crystals*, Cambridge University Press: Cambridge, 1987. (b) Pope, M.; Swenberg, C. E. *Electronic Processes in Organic Crystals*; Oxford University Press: Oxford, 1982.